Toluene pyrolysis using high-repetition-rate shock tube coupled to synchrotron-based double imaging photoelectron/photoion coincidence spectroscopy

F. E. Cano Ardila[1], S. Nagaraju[1], R. S. Tranter[2], A. W. Jasper[2], S. Abid[1], A. Desclaux[1], A. Roque Ccacya[1], L. Nahon, G. A. Garcia[3], N. Chaumeix[1], A. Comandini[1]

[1]Institut de Combustion, Aérothermique, Réactivité et Environnement, CNRS-INSIS UPR-3021, Orléans, France

[2]Chemical Sciences and Engineering Department, Argonne National Laboratory, Illinois USA

[3]Synchrotron SOLEIL, L'Orme des Merisiers, St. Aubin BP 48, 91192 Gif sur Yvette, France

1   Introduction

Toluene (C_7H_8) is a monoaromatic hydrocarbon that can be found in jet propellants and gasolines. Additionally, it is considered as an important fuel surrogate component and intermediate during the formation and growth of PAHs. Several speciation works on toluene pyrolysis using flow reactors and conventional shock tubes coupled to gas chromatographic systems highlighted possible reaction pathways for the formation of PAHs at both low pressures [1]–[3] and high pressures [4],[5]. The most recent study on toluene pyrolysis using a single pulse shock tube (SPST) coupled to GC/MS was performed at engine like conditions with detection of several PAH molecules up to four rings [6]. More importantly, the experiments served to the development of a detailed PAH chemical kinetic model that was validated and compared against other well established models available in the literature [7]. The measurements showed the presence of major products including fluorene (m/z 166), phenanthrene/anthracene (m/z 178), acenaphthylene (m/z 152) and minor products like m/z 202 which was mainly attributed to the four-ring products pyrene and fluoranthene. On the other hand, the limitations of the conventional laboratory-based methodologies (condensation of heavy products, limited sensitivity and isomer selectivity) do not allow a comprehensive investigation of the large PAHs towards the soot nucleation. The present pyrolytic study on toluene chemistry using the miniature high-repetition-rate shock tube developed at ICARE (ICARE-HRRST) with double-imaging photoelectron/photoion coincidence spectroscopy (i²PEPICO) implements up-to-date kinetic techniques to improve our fundamental understanding on the formation of PAH products, including detection of large multi-ring structures and complex isomer identification supported by the measurement of experimental mass-selected photoelectron spectra (PES) and the use of new ab-initio PES calculations.

2   Experimental set-up

Our previous work on ethanol pyrolysis [8] provided a thorough overview of the operation and results of the ICARE-HRRST/i²PEPICO combination as implemented at the beamline DESIRS of synchrotron SOLEIL [9]. Only a brief overview is presented here. Part of the 8 mm i.d driven section of the HRRST is fitted into the primary vacuum chamber (SAPHIRS) and supported on rails for simple mounting and demounting. This part includes the end-wall with the nozzle, the four venting valves, and two 60 mm intermediate sections. When SAPHIRS is in operation, the vacuum level is between 10^{-6} and 10^{-3} mbar. The fill valve and the high-pressure solenoid valve are located just outside the main chamber. The interface between the inside and the outside of SAPHIRS is made through an 8 mm i.d. tube and a bellow which allows the shock tube to move as necessary for alignment purposes. Indeed, the chamber where the HRRST sits can be mechanically moved to guarantee the alignment between the two skimmers which form the double stage pumping system. On the other hand, the alignment between the HRRST nozzle and the first skimmer is obtained by means of a "bird cage" attached to the skimmer holder. The end of the cage is machined to accept the end-section of the miniature shock tube. The concentricity of the parts is < 0.01 mm and thus axial alignment of the nozzle and the skimmer is ensured. Compared to the previous design, the new cage allows the distance between the nozzle tip and the skimmer tip to be easily varied. With the first and second skimmer orifices equal to 1 and 2 mm respectively, and with a nozzle orifice of 400 μm, the optimal distance between the nozzle and the skimmer tips is found to be around 9.5 mm. This distance allows the pressure inside the mass spectrometer chamber to remain at acceptable levels even when the shock tube runs at 1.5 Hz (between 10^{-8} and 10^{-6} mbar during operation). Despite this, all the experiments presented here are performed at 1 Hz repetition rate.

Two different operation modes of data acquisition from the DELICIOUS mass spectrometer were implemented. The first is identical to the mode used in ref. [8], where for each HRRST run a trigger signal is sent to the mass spectrometer control computer which acquires data for an 8 ms time span ("pulsed mode"). Each run is associated with specific ions/electrons arriving at the detectors as function of time, thus the kinetics can be extracted from the raw data. On the other hand, as also noticed in [8], due to the specific pulsed character of the HRRST operation accurate PES curves can be obtained only for species with relatively high concentrations. In order to overcome this limitation, a second mode of acquisition was tested ("continuous mode"). In this case, the data are continuously saved and averaged, so that higher signals could be obtained. Of course, there is no possibility to have kinetic information in this second mode. In particular, the pulsed mode was used with photon energy of 10 eV, so that the fuel as well as the main aromatic intermediates could be measured, while the work in continuous mode with photon energy of 8.5 eV, thus focusing specifically on the PAH species whose typical ionization energies are below 8.5 eV. More than 110 500 experiments were averaged in the pulsed mode ($T_5 = 1362\pm22$ K and $P_5 = 6.6\pm0.2$ bar), while around 46 500 in continuous mode ($T_5 = 1351\pm13$ K and $P_5 = 6.4\pm0.1$ bar). All the experiments were performed with mixtures composed of 0.1% toluene in argon bath gas.

3   Results and discussion

The average mass spectrum over the 8 ms acquisition time in pulsed mode is presented in Figure 1. The figure is divided into four panels for clarity, starting from small mass to charge ratio (m/z) peaks from the decomposition of the aromatic fuel up to m/z 350 ($C_{28}H_{14}$ isomers, e.g. six-ring compounds). For all these compounds, kinetic profiles as function of the temperature can be derived from the raw mass spectrometer data. In reality, signals could be detected up to a m/z ratio of 426, corresponding to $C_{34}H_{18}$, e.g. nine-ring structures, but the signal is too weak to obtain the kinetic information for m/z greater than 350. The analyses of all the toluene pyrolysis product is not trivial, and it requires understanding of the relative importance of the different growth pathways. As a general procedure, reactions involving relatively small molecules are selected as reference reactions for extrapolation to larger systems. In the present case, the detailed analyses of the isomeric distributions for major m/z intermediates based on the PES measurements in continuous mode will provide further insides together with kinetic analyses with literature model [6]. The experimental PESs together with the convolved curves obtained summing

single contributions from different isomers are shown in Figure 2. The single profiles are from literature PES measurements or ab-initio theoretical calculations.
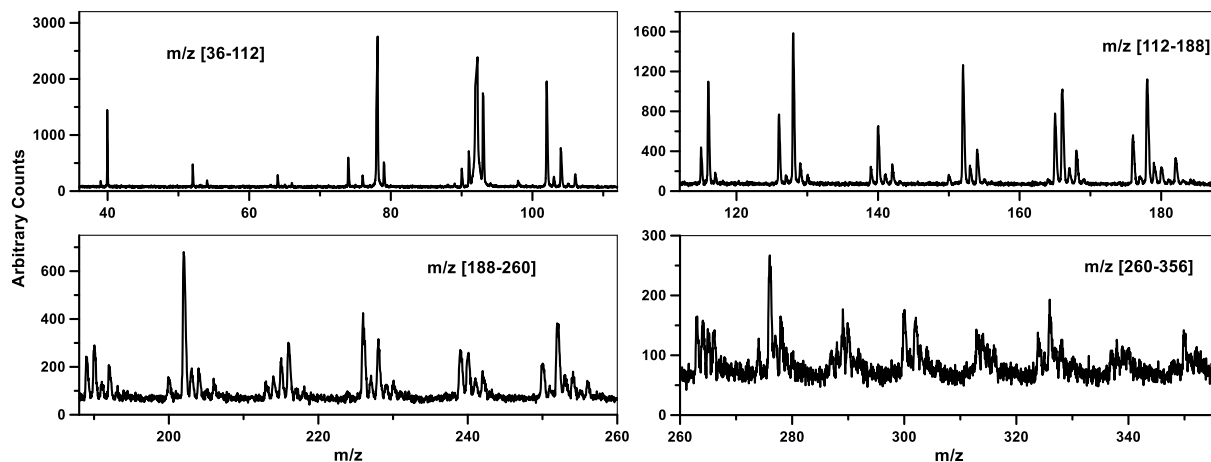
Figure 1. Mass spectrum obtained in pulsed mode, averaging over 110 500 experiments. 0.1% toluene in argon, photon energy 10 eV.
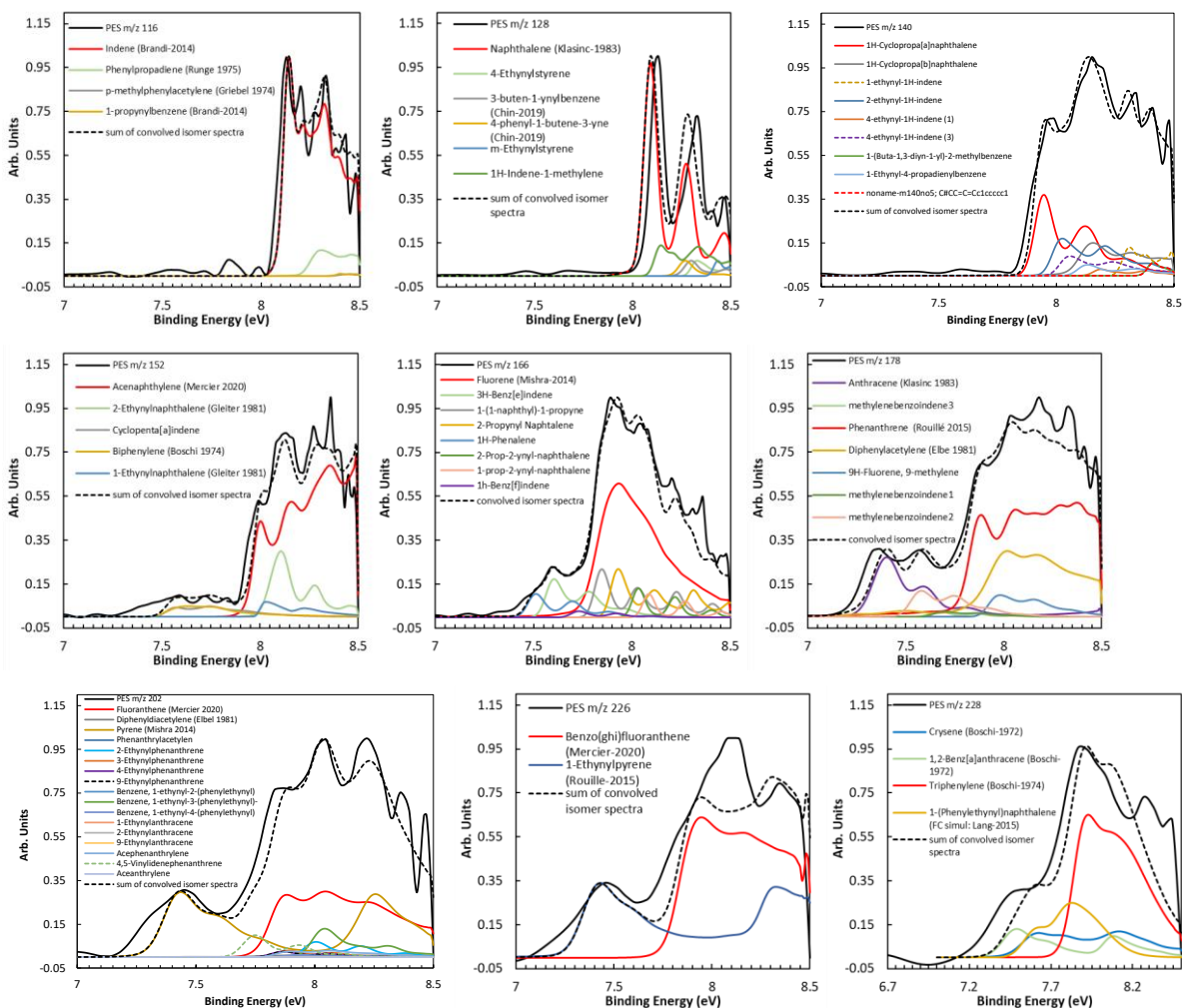
Figure 2. Selected photoelectron spectra.

Among the two-ring structure, indene is the main compound with m/z 116 (~88% contribution), from the is mainly produced from the reaction between the benzyl radical (C_7H_7) and acetylene (C_2H_2) as well the isomerization of $C_6H_5C_3H_3$ isomers. Among the $C_6H_5C_3H_3$ isomers, a relatively small amount of phenylpropadiene ($C_6H_5CHCCH_2$) contributes to the signal (around 10%). Phenylpropadiene is produced from the reaction of C_3H_3 with phenyl (C_6H_5). Concerning m/z 128, naphthalene (70% contribution) is produced mainly by the cycloaddition fragmentation (CAF) mechanism where o-benzyne comes from the direct fragmentation of the fuel radical ($C_7H_7 = o\text{-}C_6H_4+CH_3$). Other pathways involve the recombination between the naphthyl radicals and H, the H-abstraction by the naphthyl radicals to toluene, and the dehydrogenation and ring-rearrangement steps from methyleneindanyl ($C_9H_7CH_2$), the radical of 1-methylindene ($C_9H_7CH_3$), and from the $CH_3C_9H_6$ radical. 1-Methylindene was also observed at m/z 130. The naphthyl radicals derive mainly from the reaction between C_6H_5 and C_4H_2, while the $C_9H_7CH_2$ and the $CH_3C_9H_6$ radicals from stepwise pathways starting from the fuel radicals, C_7H_7 and $C_6H_4CH_3$ respectively, reacting with the propargyl radical. Among the minor isomers, 1H-indene-1-methylene contributed by ~10%. 1H-Indene-1-methylene comes from the fragmentation of methyleneindanyl ($C_9H_7CH_2$) and $CH_3C_9H_6$. The following major peak is m/z 140. This is quite surprising, as previous speciation studies did not identify such compounds. Among the various isomers, cyclopropanaphthalene isomers ($C_{10}H_6cyCH_2$) are the main contributors (around 46% of the total signal), from the reactions of naphthalene structures with CH_3 moieties. Other major isomers include the ethynyl-1H-indenes (38% total contribution), from the reactions of the indene radicals with C_2H_2. Acenaphthylene is generally recognized as one of the main PAH products in pyrolytic studies, as an intermediate of the HACA route. Also in this study, the major m/z 152 isomer is acenaphthylene (61%). Based on the kinetic analyses, acenaphthylene is formed mainly from the pathway through the formation of biphenyl (from $C_6H_5+C_6H_6$, $C_6H_5+C_6H_5$) followed by H-abstraction to the biphenyl radical or directly to the biphenyl radical (from $C_6H_5+o\text{-}C_6H_4$) followed by isomerization reactions, with only a minor contribution from the HACA route. Another minor pathway involves addition reactions of indenyl radical (C_9H_7) with the propargyl radical (C_3H_3). 2-Ethynylnaphthalene, produced from the reaction of the 2-naphthyl radical with acetylene, is also present in considerable amounts (25% contribution). The 1-ethynylnaphthalene contributes much less to the convolved spectrum as the reaction between 1-naphthyl radical with acetylene mainly leads to acenaphthylene. Finally, a small contribution from biphenylene and/or cyclopenta[a]indene is present, although the two PESs are very similar and can not be easily distinguished.

Concerning larger PAHs, a large peak is present in Figure 1 at m/z 166. This peak corresponds mainly to fluorene (39% contribution), formed from the recombination of fuel radical benzyl with phenyl ($C_7H_7 + C_6H_5$) and subsequent ring closure/dehydrogenation of diphenylmethane ($C_6H_5CH_2C_6H_5$), as well as, in minor importance, from the dehydrogenization of $C_{13}H_{11}$ from the reaction between the benzyl radical and m-benzyne. Various isomers present in smaller amounts are also identified. 1H-Phenalene and 3H-benz[e]indene contributes to the signal below 7.7 eV. 1H-Phenalene derives mainly from the ring-expansion of $C_{12}H_7CH_2$, while 3H-benz[e]indene from the reaction of 1-methylnaphthalene radical ($C_{10}H_7CH_2$) with acetylene. Addition of a small amount of 1h-benz[f]indene helped improving the fit in the curvature around 7.7 eV, while the contribution from 1-(1-naphthyl)-1-propyne ($1\text{-}C_{10}H_7CCCH_3$) provided the signal necessary to complete the shoulder located at around 7.84 eV, just before the biggest peak corresponding to fluorene. The corresponding 2-propynyl naphthalene ($2\text{-}C_{10}H_7CCCH_3$) is also present in considerable concentrations. The photoionization energy is very similar to the one of fluorene, but its contribution is mainly essential to fit experimental features at higher energies. These species are produced by the reactions of the 1-,2-naphthyl radicals with propyne and the 1-,2-ethynylnaphthalenes with the methyl radical. Two additional isomers were employed to improve the fitting of the region near the second highest experimental peak, 2-prop-2-ynyl-naphthalene ($2\text{-}C_{10}H_7CH_2CCH$) and 1-prop-2-ynyl-naphthalene ($1\text{-}C_{10}H_7CH_2CCH$); these two isomers are formed from the reactions of the naphthyl radicals with C_3H_3 and C_3H_4. The contributions from the minor isomers are between 7% and 14%, with exception of 1h-benz[f]indene which is present in smaller amounts (2% contribution). Concerning other three-ring structures corresponding to m/z 178, anthracene, phenanthrene, diphenylacetylene, and 9H-

fluorene, 9-methylene are the main products (contributions equal to 20%, 38%, 22%, 7%, respectively). According to the model developed in previous shock tube works on toluene pyrolysis, phenanthrene can be produced mainly from three routes. The first route involves the isomerization of anthracene, followed by the recombination reaction between two toluene radicals ($C_6H_4CH_3$), and the isomerization fragmentation of $C_{13}H_9CH_2$. $C_{13}H_9CH_2$ is mainly formed from the reaction of the benzyl radical with the fullvenallenyl radical (C_7H_5) and in a minor way from a combination between fluorenyl radical ($C_{13}H_9$) with methyl (CH_3). A minor contribution to phenanthrene comes from the composition of $C_6H_5CCHC_6H_5$ (from subsequent dehydrogenizations of bibenzyl). Anthracene is mainly produced from the recombination of toluene radicals ($C_6H_4CH_3$) with benzyl radical ($C_6H_5CH_2$). Diphenylacetylene ($C_6H_5CCC_6H_5$) is mainly produced from the dehydrogenization of bibenzyl and then $C_6H_5C_2H_2C_6H_5$, and only from a minor contribution by combination of phenylacetylene (C_8H_6) with phenyl (C_6H_5). 9H-fluorene, 9-methylene from the reaction of fluorene with CH_3 radical and subsequent dehydrogenization.

Larger PAH products were also detected and identified based on the corresponding photoelectron spectra. Pyrene and fluoranthene (20% and 32% contributions, respectively) are the main components for m/z 202, as in previous literature speciation studies [6]. These $C_{16}H_{10}$s mainly result from the recombination of phenyl (C_6H_5) with naphthyl ($C_{10}H_7$) and benzyl radical (C_7H_7) with indenyl radical (C_9H_7). The HACA route through phenanthrenyl ($C_{14}H_9 + C_2H_2$) is also possible although not the main pathway. Other major contributions come from benzene, 1-ethynyl-3-(phenylethynyl)- (from HACA step of diphenylacetylene), and 4,5-vinylidenephenanthrene (phenanthrene isomer). The presence of benzo(ghi)fluoranthene and 1-ethynylpyrene is confirmed from the analysis of m/z 226, although other unknown isomers could contribute to the experimental PES. In particular, 1-ethynylpyrene highlight the HACA step from pyrene. Finally, triphenylene is the major m/z 228 compound (57% contribution), together with 1-(phenylethynyl)naphthalene ($C_{10}H_7CCC_6H_5$, 22% contribution). The chemistry of these four-ring intermediates still need to be fully clarified, although addition of o-benzyne to biphenyl has been proposed in the past as source of triphenylene, while 1-(phenylethynyl)naphthalene should come from the reaction between the 1-naphthyl radical with phenylacetylene. Other minor isomers include crysene and 1,2-benz[a]anthracene (10-11% contribution).

Based on the results discussed in the previous paragraphs, several common pathways can be identified, including the HACA route, the addition of resonantly stabilized radicals (C_3H_3, C_7H_7), addition of the phenyl radical, methylation, and diacetylene addition to aromatic radicals. By integrating the peak in Figure 1, the general exponential trend in terms of signal response for the different m/z can be obtained as in Figure 3. In particular, the HACA route is highlighted as the main pathway for the growth of large PAHs, as the major peaks are separated by m/z 24 and 26 (corresponding to acetylene addition to aromatic radicals followed by H-elimination or formation of a ring after H addition, respectively). Examples of possible species formed by HACA route are also presented in Figure 3. Detailed analyses of the other main growth reaction mechanisms based on the major and minor products will be presented.
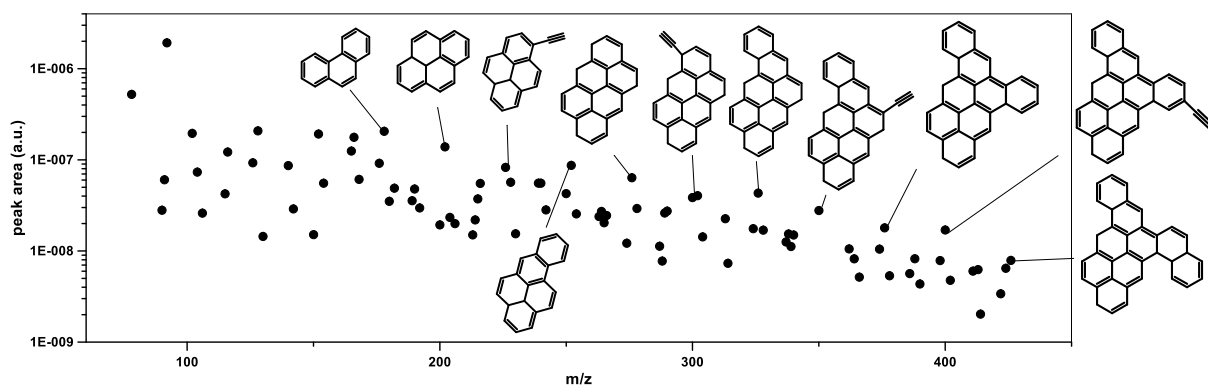
Figure 3. Integrated peaks from mass spectrum in Figure 1.

Acknowledgment

References

[1]   B. Shukla, A. Susa, A. Miyoshi, and M. Koshi, "In situ direct sampling mass spectrometric study on formation of polycyclic aromatic hydrocarbons in toluene pyrolysis," *J. Phys. Chem. A*, vol. 111, no. 34, pp. 8308–8324, 2007.

[2]   T. Zhang *et al.*, "An experimental and theoretical study of toluene pyrolysis with tunable synchrotron VUV photoionization and molecular-beam mass spectrometry," *Combust. Flame*, vol. 156, no. 11, pp. 2071–2083, 2009.

[3]   W. Yuan, Y. Li, P. Dagaut, J. Yang, and F. Qi, "Investigation on the pyrolysis and oxidation of toluene over a wide range conditions. I. Flow reactor pyrolysis and jet stirred reactor oxidation," *Combust. Flame*, vol. 162, no. 1, pp. 3–21, 2015.

[4]   M. B. Colket and D. J. Seery, "Reaction mechanisms for toluene pyrolysis," *Symp. Combust.*, vol. 25, no. 1, pp. 883–891, 1994, doi: 10.1016/S0082-0784(06)80723-X.

[5]   R. Sivaramakrishnan, R. S. Tranter, and K. Brezinsky, "High pressure pyrolysis of toluene. 1. Experiments and modeling of toluene decomposition," *J. Phys. Chem. A*, vol. 110, no. 30, pp. 9388–9399, 2006, doi: 10.1021/jp060820j.

[6]   W. Sun, A. Hamadi, S. Abid, N. Chaumeix, and A. Comandini, "Probing PAH formation chemical kinetics from benzene and toluene pyrolysis in a single-pulse shock tube," *Proc. Combust. Inst.*, vol. 38, no. 1, pp. 891–900, 2021.

[7]   W. Pejpichestakul *et al.*, "Examination of a soot model in premixed laminar flames at fuel-rich conditions," *Proc. Combust. Inst.*, vol. 37, no. 1, pp. 1013–1021, 2019.

[8]   S. Nagaraju *et al.*, "Pyrolysis of ethanol studied in a new high-repetition-rate shock tube coupled to synchrotron-based double imaging photoelectron/photoion coincidence spectroscopy," *Combust. Flame*, vol. 226, pp. 53–68, 2021.

[9]   G. A. Garcia, B. K. Cunha de Miranda, M. Tia, S. Daly, and L. Nahon, "DELICIOUS III: A multipurpose double imaging particle coincidence spectrometer for gas phase vacuum ultraviolet photodynamics studies," *Rev. Sci. Instrum.*, vol. 84, no. 5, p. 53112, 2013.